Heliyon

Received:
24 October 2018
Revised:
23 February 2019
Accepted:
11 April 2019

Cite as: Abhay Agrawal, R. S. Rana. Theoretical and experimental performance evaluation of single-slope single-basin solar still with multiple V-shaped floating wicks.
Heliyon 5 (2019) e01525.
doi: 10.1016/j.heliyon.2019.e01525

Theoretical and experimental performance evaluation of single-slope single-basin solar still with multiple V-shaped floating wicks

Abhay Agrawal [a,*], **R. S. Rana** [b]

[a] *Department of Mechanical Engineering, Rewa Engineering College, Rewa, MP, India*

[b] *Department of Mechanical Engineering, Maulana Azad National Institute of Technology, Bhopal, MP, India*

[*] Corresponding author.

E-mail address: abhayagrawalgec@gmail.com (A. Agrawal).

Abstract

A solar still is used to convert saline water into potable water by means of the distillation process. In order to improve the productivity of conventional solar still, various modifications are implemented by researchers. In the present study, multiple V-shaped floating wicks are used to enhance heat absorption and thereby increase productivity. The experiments are performed during the summer and winter seasons in Rewa, India (Latitude: 24.5373° N; Longitude: 81.3042° E). These multiple floating wicks are made from black jute cloth wrapped in V-shaped pieces of thermocol. Because of their V-shaped profile, the evaporative surface area of modified solar still is 26% larger than that of conventional solar still. The maximum daily productivity in one of the clear days is found to be approximately 6.20 kg/m^2 in summer and 3.23 kg/m^2 in winter with daily efficiencies of 56.62% and 47.75%, respectively. A theoretical thermal model is formulated by using the energy balance equations of the modified solar still. Reasonable agreement was seen between the theoretical and experimental results of modified solar still. An economic analysis is also performed for the modified solar still and conventional solar still; in a 10-year life cycle, the annual cost of

https://doi.org/10.1016/j.heliyon.2019.e01525

distilled water is estimated at Rs. 1.81/kg for the former and Rs. 2.24/kg for the latter.

Keywords: Mechanical engineering, Energy

1. Introduction

God has provided humans with a variety of natural gifts. Among life's essentials, water is critical; many regard it as life itself. Practically two-thirds of the human body is made up of water, and humans cannot survive without it. Countless living organisms depend on it to thrive; evidently, an adequate water supply is crucial. Water is abundant and covers two-thirds of the earth's surface. In reality, however, 97.4% of this vast amount of water is saltwater found in the oceans. The salinity of seawater is extremely high (3000−35 000 parts per million (PPM)) and exceeds the permissible water salinity limit (less than 500 PPM) prescribed by the World Health Organization [1]; hence, it is not potable. Moreover, 1.8% of earth's water is frozen in the polar caps. The drinking water that we consume daily is barely 0.8% of what we source from rivers, ponds, lakes, and underground water. Moreover, because of the rising population and pollution, drinking water from these sources can potentially afflict two billion of the world's population with water-borne diseases, such as polio, jaundice, mild fever, cholera, diarrhea, tuberculosis, dysentery, encephalitis, and conjunctivitis; clearly, potability is compromised.

In the last century, because living standards have highly improved, the increase in water utility is more than twice the increase in population. In 2015, the global population was 7.3 billion; 54% of this number live in rural areas and 663 million of them lack water sources. It is presumed that by 2025, 1800 million people from different countries will experience water scarcity. India accounts for only 4% of the world's freshwater resources but 16% of the world's population. Based on the 2011 population census in India, of the total 1200 million population, providing drinking water to approximately 800 million people in the rural areas will be extremely difficult [2]. The geographical location of India is between 7° and 37° latitude; moreover, India receives an average solar radiation of 16 700−22 960 kJ/m^2/d. Because of abundant solar radiation available throughout the year, the conversion of brackish water to potable water by means of the solar distillation process can easily satisfy the drinking water requirement of rural India.

Water can be purified at a considerably low cost when the solar distillation process is used because thermal energy is supplied by solar energy. The impure water evaporates when it receives solar energy; subsequently, water vapor separates from the dissolved matter and condenses in the form of pure water. Solar distillation is an established process for purifying saline water using radiant energy from the sun

https://doi.org/10.1016/j.heliyon.2019.e01525

because it is charge-free and pollution-free; moreover, solar energy is unlimited and abundant in all parts of India.

Solar still is a device in which the solar distillation process occurs, and is suitable for the low-cost production of potable water in rural areas. Solar still can be constructed from locally available materials. Solar still is a rectangular black-painted box that contains impure water and tightly covered by glass cover. The water contained in the basin box is evaporated by the heat of solar rays; it is collected as pure water in the form of condensate. Solar still and its maintenance is inexpensive; hence, it is an excellent device to obtain potable water in remote areas.

Compared with other conventional distillation systems, the productivity and efficiency of solar still are considerably lower. Several attempts have been made by researchers to improve the performance of solar still by providing additional evaporating surface. Moreover, researchers around the world have developed several modified designs for different climatic and operating parameters to enhance the performance of solar still.

Dunkle [3] has provided the heat and mass transfer equations for various heat transfer coefficients (convective and evaporative) of conventional solar still. The main disadvantage of conventional solar still is its low productivity. Therefore, researchers have made several modifications, such as increasing the evaporation area by using jute cloth, wick, sponges, and different heat storage materials. Multiple wicks solar still was developed by Sodha et al. [4]; in this still, the blackened wet jute cloth was used to increase the evaporation rate. The obtained overall efficiency and distillate output on winter days in Delhi were 34% and 2.5 L/m^2/d, respectively. Al-Karaghouli and Minasian [5] compared the experimental daily distillate outputs of tilted wick, floating blackened jute wick, and conventional basin-type solar stills. It was found that the floating blackened jute wick solar still produced a higher distillate output than the tilted wick and conventional solar stills; its output was 10.5 L/m^2 for the same outdoor environmental conditions. Naim and Kawi [6] modified conventional solar still by using charcoal particles as a heat absorber medium on the wick surface. Compared to the wick-type stills, a productivity improvement of approximately 15% was reported. Abu-Hijleh and Rababa'h [7] increased the distillate output in basin water by using yellow and black sponge cubes as well as black steel cubes and coal cubes; sponge cubes were found to be more effective. The distillate output of the still with cubes increased from 18% to 273% compared to that of conventional still.

The theoretical (theo.) and experimental (exp.) performances of multi-wick solar stills (single and double slopes) were conducted by Shukla and Sorayan [8]. Analytical equations were derived, and a computer model was developed for the proposed solar still. A fair agreement was found between the theoretical and experimental results. Janarthanan et al. [9] analyzed the performance of a new design of corrugated

https://doi.org/10.1016/j.heliyon.2019.e01525

floating cum tilted-wick solar still with a flowing water effect over the condensing cover. Energy balance equations were derived, and a thermal model of the considered solar still was developed. It was concluded that the experimental results approximated the theoretical results. Moreover, the significant effect of the water flowing over the condensing cover was observed on the thermal performance of a corrugated floating cum tilted-wick solar still. Sakthivel et al. [10] performed experiments by using jute cloths placed at the middle and the rear wall of a conventional solar still. It was found that the daily productivity of the still increased by 20% compared to the conventional still. By this modification, the still's efficiency increased from 44% to 52%.

Murugavel and Srithar [11] investigated the performance of a double-slope basin-type solar still with various wick materials, such as light black cotton cloth, light jute cloth, sponge sheet, waste cotton pieces, and coir mat. Multiple combinations of aluminum rectangular fins covered with different wick materials were also investigated. Among the materials tested, the light black cotton cloth produced the maximum daily distillate output. The longitudinal arrangement of rectangular aluminum fins with cotton cloth was found to be more effective. Srivastava and Agrawal [12] conducted theoretical and experimental studies and modified the design of conventional solar still by using porous absorbers of low thermal inertia; blackened jute cloth pieces were used as porous absorbers. The modified still was 68% more productive on clear days. During cloudy days, however, the distillate output was approximately 35% more than conventional still.

Manikandan et al. [13] presented a review on various wick-type solar still designs, such as wick-basin type, floating wick type, multi-wick type, floating cum tilted-wick type, tilted-wick type, and concave wick-type solar stills; maximum productivity was observed in the floating wick-type solar still. Matrawy et al. [14] modeled and conducted experimentations on modified forms of basin type solar stills. In their model, the corrugated black cloths on the porous material were immersed in water; the cloths absorbed the water as a result of capillary effect. The distillate output of the modified solar still increased by approximately 34% than that of conventional still. Omara et al. [15] studied the performance of conventional solar still (CSS) and corrugated solar still (CrSS) with layered wick materials and reflectors. The results showed that the productivity of the modified solar still for a 1-cm brine depth was 145.5% more than that of conventional solar still. The daily efficiency values of modified and conventional solar stills were approximately 59% and 33%, respectively.

Samuel et al. [16] conducted theoretical and experimental works on increasing the distillate output using different energy storage materials. It has been observed that the solar still with spherical salt balls produced the maximum distillate output of 3.7 kg/m^2/d than the conventional still with sponge (2.7 kg/m^2/d) and that without

https://doi.org/10.1016/j.heliyon.2019.e01525

any storage material (2.2 kg/m^2/d). The experimental performance evaluation of V-corrugated absorber solar still with and without phase-change material (PCM; in this case, paraffin wax) was presented by Shalaby et al. [17]. It was inferred that the daily productivity values of V-corrugated absorber solar still with PCM were 12% and 11.7% higher than those of the V-corrugated absorber solar still without PCM and the V-corrugated absorber solar still with PCM and wick, respectively. The modified basin-type double-slope multi−wick solar still was proposed by Pal et al. [18]. A number of experiments was performed on the modified double-slope solar still; the daily productivity values obtained were 4.50 and 3.52 L/m^2 for black cotton wicks and jute wicks, respectively, at a 2-cm basin water depth. Agrawal et al. [19] presented the experimental and theoretical comparisons of productivity and heat transfer coefficients of conventional still under Indian conditions for various basin water depths (2−10 cm). It was found that as the basin water depth increases, the distillate output decreases. For 2-cm and 10-cm basin water depths, the theoretical and experimental daily efficiency values were approximately 52.83% and 41.75%, and 41.49% and 32.42%, respectively.

Panchal and Mohan [20] reviewed various methods in increasing the distillate output in solar still. Numerous approaches that previous researchers utilized were presented; moreover, the results of different still designs with fins, various energy storage materials, and multi-basins were compared.

Panchal and Patel [21] studied the impact of operational and climatic parameters on the yield of solar still. The experimental performance of a single-basin vertical multiple-effect diffusion solar still with floating cotton wick and heat recovery system was evaluated by Kaushal et al. [22]. The study found that the daily productivity of the modified still was 21% higher than that of the reference still (without floating wick and heat recovery system). Sellami et al. [23] improved the performance of a single-basin solar still by using blackened sponge sheets with different thicknesses pasted over the basin liner (heat-absorbing surface). The productivity values of solar still increased by 57.77% and 23.03% for the 5-mm and 10-mm thick sponge sheets, respectively; however, for the 15-mm thick sponge sheet, the productivity value was 29.95% less than that of conventional still. Sharon et al. [24] evaluated the performance of tilted solar still with wick and basin; they found that the daily distillate output values were 4.99 and 4.54 L/m^2/d, respectively. Haddad et al. [25] introduced vertical rotating wick to basin-type solar still to improve their performance. It was observed that the daily distillate output values were 5.03 kg/m^2 in winter and 7.17 kg/m^2 in summer.

Panchal et al. [26] conducted theoretical and experimental studies on solar stills with marble pieces and sandstones as heat energy storage materials; moreover, they investigated the effect of cooling and dripping arrangements on these stills. It was found that compared to that of conventional still, the distillate output values of solar still

https://doi.org/10.1016/j.heliyon.2019.e01525

with sandstones and marbles increased by 30% and 14%, respectively. With the further use of cooling and dripping arrangements, the distillate output increased by 12%. Experiments were performed by Vala et al. [27] to compare the operational parameters of pyramid-shaped still and single-slope conventional still with and without jute cloth. In a lower basin water depth, the distillate output value of the pyramid-shaped still was 26% more than that of the single-slope still; moreover, the application of jute cloth enhanced the efficiency of both stills.

Manokar et al. [28] compared the thermal performance of an inclined solar panel basin solar still with active and passive modes. It was observed that the daily productivity obtained in the active mode is 44.63% higher than that in the passive mode. The productivity values in the active and passive modes of solar still were 7.91 and 4.38 kg/m^2/day, respectively. Kabeel et al. [29] improved the productivity of conventional basin solar still by using the knitted jute cloths that are wrapped around the sand heat energy storage. The distillate output values of solar still with and without modifications were found to be 5.9 and 5 kg/m^2/day, respectively, at a 20-kg basin water mass. Shanmugan et al. [30] enhanced the thermal performance of a single basin solar still by introducing PCMs, nanoparticles (Al_2O_3), and various basin wick materials. It was observed that from 9:00 a.m. to 5:00 p.m. the distillate output values of single basin solar still (fin with cotton wick) with PCMs and nanoparticles were 7.460 and 4.120 kg/m^2 during summer and winter, respectively.

Experimentations were performed by Rashidi et al. [31] to enhance thermal performance by introducing reticular porous media (black sponge rubber) to solar still. It was observed that the productivity of the modified still was 17.35% higher than that of the conventional solar still. The single-basin single-slope solar still was modified by Arunkumar et al. [32] by using a porous absorber (carbon-impregnated foam) and bubble-wrap insulation. It was found that the daily productivity values of the solar still without bubble-wrap insulation, with bubble-wrap insulation, with both porous absorber and bubble-wrap insulation, and with wooden insulation only are 1.9, 2.3, 3.1, and 2.2 L/m^2, respectively. Abdullah et al. [33] designed, fabricated, and investigated the performance of six wicks solar still with humidification and dehumidification units. The experiment was conducted at different water flow rates in the inclined solar still; different packing materials were used in the humidifier. The distillate output value at a flow rate of 4 kg/min was higher than that at 2 kg/min. Modi and Modi [34] examined the performance of single-slope double-basin solar stills using jute and black cotton cloths (wick material) placed as a small pile over the absorber plate of solar stills. The experimental results revealed that at basin water depths of 0.01 and 0.02 m, the distillate output values of the solar still with small pile of jute cloth are 18.03% and 21.46% higher than that of a solar still with a small pile of black cotton cloth, respectively.

https://doi.org/10.1016/j.heliyon.2019.e01525

In the present work, theo. and exp. analyses are conducted to evaluate the thermal performances of two solar still units during the clear days of summer and winter seasons. The first unit is a conventional single-slope single-basin solar still (CSS), which is used as a base unit and is completely synchronized. The second unit is the modified single-slope single-basin solar still (MSS), in which V-shaped floating wicks are used as absorber surfaces to enhance the amount of distillate outputs caused by the increase in evaporation surface area. The experimentations are performed to obtain the different parameters of both stills as follows: inner and outer glass temperatures (temp.); basin water temp.; wetted V-shaped floating wick temp.; convective, evaporative, radiative heat transfer coefficients; productivity; efficiency. The theo. parameters are derived from the mathematical thermal models of solar stills; these models are developed based on Dunkle's relations [3] and validated by experimental results. The theo. and exp. results exhibit good agreement.

2. Experimental

2.1. Experimental setup

The exp. setup comprises two identical single-slope single-basin type solar stills. The first still unit is used as a CSS, whereas the second is modified into a V-shaped floating wick design. The line diagram and photograph of the exp. setup of an MSS are presented in Figs. 1 and 2. Both stills are in the shape of a rectangular box (0.80 $\times$ 0.65 $\times$ 0.20 m^3) and are made of 0.001-m thick rustproof galvanized iron sheets. Each of the stills are put in a plywood box with a single layer of a 0.008-m expanded

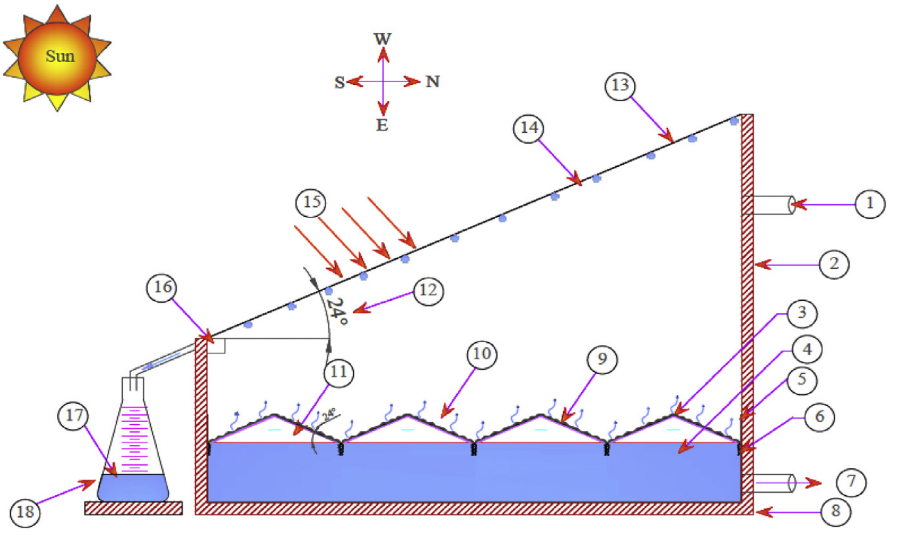

Fig. 1. Line diagram of MSS. (1) Water inlet (2) Sidewall (3) V-type floating wick (4) Impure water (5) Insulation (6) G.I. basin painted black (7) Impure water outlet (8) Outer box (plywood) (9) Black jute cloth (10) Evaporated water vapor (11) Thermocol (12) Glass cover angle (13) Glass cover (14) Condensate droplet (15) Solar radiation (16) Distillate channel (17) Distillate output (18) Measuring jar.

https://doi.org/10.1016/j.heliyon.2019.e01525

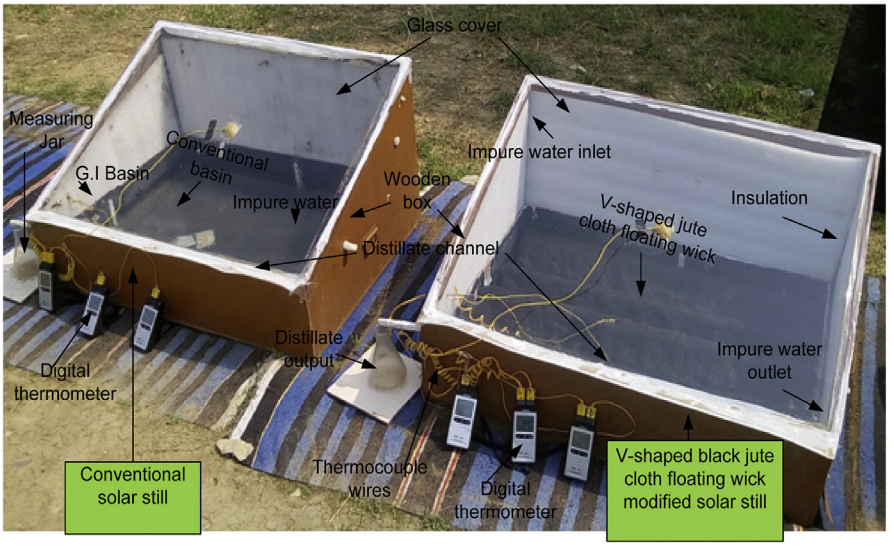

Fig. 2. Photograph of experimental setup of solar stills.

polyethylene sheet insulation, which reduces heat losses from solar stills. To enhance the capacity for absorbing solar radiation, the interior surfaces of the metallic basin box is painted in black. Each of the solar stills are covered with a 0.004-m ordinary glass sheet, which is fitted on the top edges of the plywood frame with a glass cover that is horizontally inclined at 24° [35] (approximately the same as the latitude of Rewa (24.5373° N)), to maximize the transmitted solar radiation and minimize heat losses at the top. All the openings and gaps between the edges of the glass cover and wooden frame are filled with silicone rubber sealant and glass putty to ensure no vapor leakage. Distillate channels made of aluminum are fitted under the lower end of each glass cover in the stills at a proper slope angle for the smooth flow of distillate outputs through the polyvinyl chloride (PVC) pipes installed inside the measuring jars. Two holes are made on the opposite sidewalls of each solar still. The 5-mm diameter PVC pipes are inserted into the holes. These pipes supply saline water to the solar stills through a controlled valve-fitted tank; water is also discharged from the basin of solar stills through these pipes during cleaning.

In the MSS, V-shaped floating wicks are used in the basin. The photograph of V-shaped black jute cloth floating wicks is shown in Fig. 3. These wicks are made of rectangular thermocol pieces with two sizes (0.790 m × 0.086 m × 0.020 m and 0.790 m × 0.157 m × 0.020 m). First, the two pieces with a shorter width (0.086 m) are joined lengthwise at the V-shaped cross-section; thereafter, the third piece with a longer width (0.157 m) is joined as a base to form an isosceles triangular cross-section bar. Both tilted surfaces are set at an angle of 24° with respect to the base in order to receive as much solar radiation as possible; this angle is the same as the glass cover inclination. Four identical floating triangular bar pieces of thermocol are prepared. The base of the triangular bar floats on the top surface of the basin

https://doi.org/10.1016/j.heliyon.2019.e01525

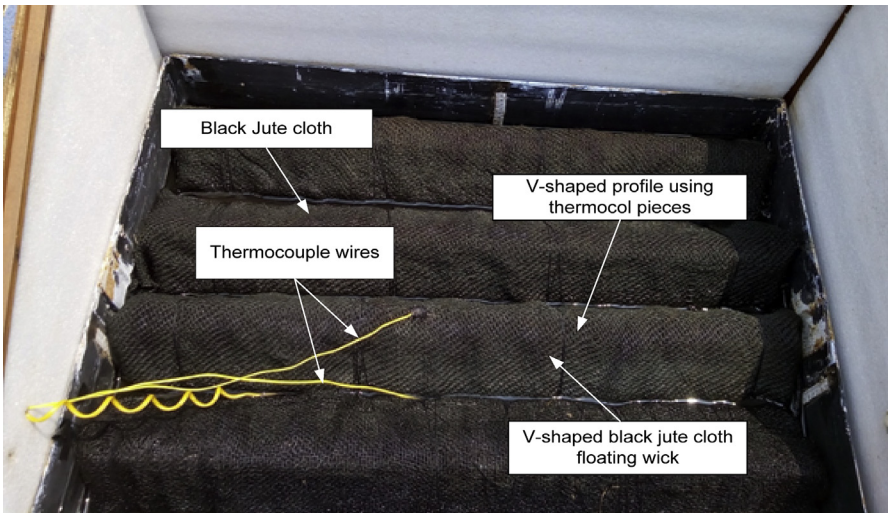

Fig. 3. Photograph of V-shaped black jute cloth floating wicks.

water, and the other two inclined surfaces face upward towards the glass cover forming a "V" shape. Furthermore, the black jute cloth is spread along the "V" shape portion, and the rest of the jute cloth remains under the basin water; the wetness of the black jute cloth maintained through capillary action. These four pieces of V-shaped floating wicks are floated side by side in the basin water along the solar still length. Therefore, the basin water surface is completely covered (proper clearance from the walls of the solar still basin). The calibrated Ni−Cr thermocouple wires are inserted through the tiny openings on the side walls of both stills. The temp. at the different locations of solar stills are measured by multichannel digital thermometer viz. glass cover temp., basin water temp., V-shaped floating wick temp. The hourly variation of global solar intensity, wind speed, and ambient air temp. are obtained from the Solar Radiation Resource Assessment (SRRA) Station at Rewa Engineering College, Rewa (M.P), India (installed by Centre for Wind Energy Technology, Chennai, India [19]). The SRRA Station is shown in Fig. 4.

2.2. Experimental procedure

The solar still experiments are conducted for several days during the clear days of summer and winter seasons at Rewa, (M. P.), India. Among these days, the best observations were recorded on April 22, 2017 (summer) and January 13, 2017 (winter). The orientation of the solar still is sustained along the east−west direction with the glass cover facing south to maximize incident solar radiation. Both the solar stills are filled up to a 2-cm basin water depth with boring water with a total dissolved solid value of 1043 mg/mL [19] obtained from a local source. Moreover, the synchronization of the MSS and CSS are tested before the experiments are performed. These are filled with the same amount of basin water, and their distillate outputs are

https://doi.org/10.1016/j.heliyon.2019.e01525

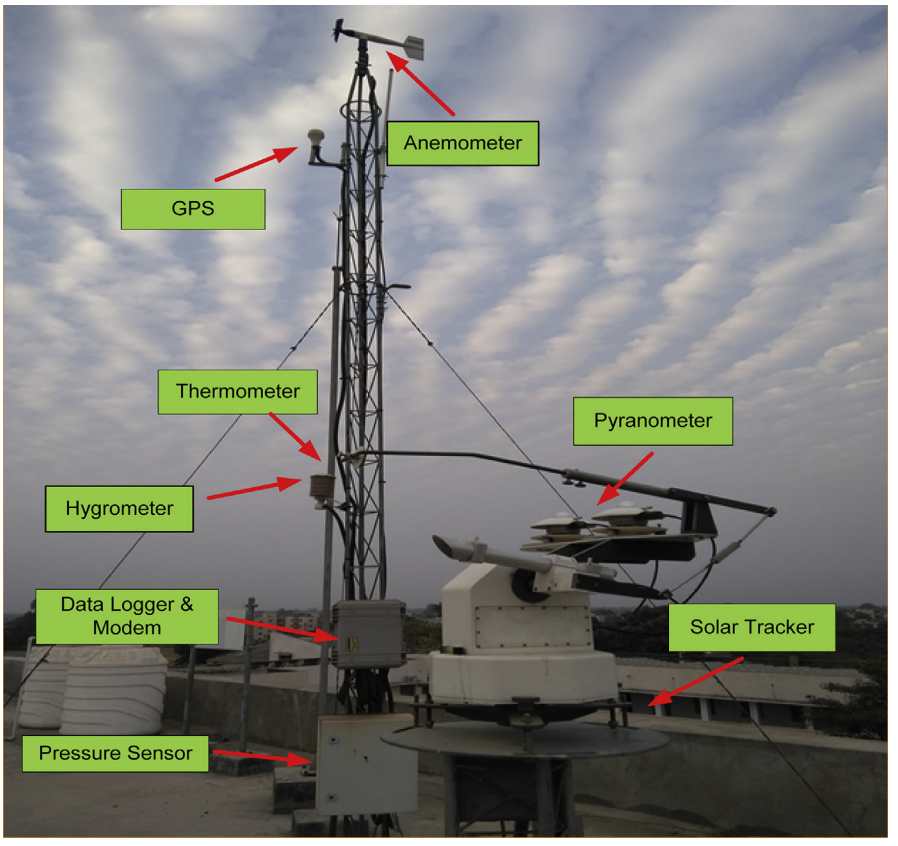

Fig. 4. Photograph of solar radiation resource assessment station Rewa.

obtained for five days. The performance results of both solar stills show good synchronization. After a synchronous performance test, experiments are conducted. All their required parameters are measured from 8:00 a.m. to 7:00 p.m. and then resumes at 8:00 a.m. the next day. In this manner, the exp. observations, including the nocturnal distillate output, are recorded for 24 h.

2.3. Experimental uncertainty analysis

Experimental uncertainty (error) always exists as a result of the measuring method, observation (reading) process, environmental conditions, and calibration and error of measuring instruments. The error in experimental readings and instruments can be represented as

$$Z = Z_{best} + \Delta e \tag{1}$$

where Z_{best} is the best estimated reading of physical quantity, and Δe is an absolute error that occurs during the experiment. The uncertainty in the experimental study can be estimated in two ways described below.

https://doi.org/10.1016/j.heliyon.2019.e01525

2.3.1. Internal uncertainty

An estimation of uncertainty is performed for the experimental observations of various parameters. The sample calculations of experimental uncertainty in each set of observations of individual parameters are conducted by Nakara and Choudhary [36] and Tiwari et al. [37]. The mathematical expression of the percentage of uncertainty is presented as

$$\text{Percentage uncertainty} = \frac{U_i}{B} \times 100 \tag{2}$$

where

$$U_i = \sqrt{\frac{\sigma_1^2 + \sigma_2^2 \ldots + \sigma_S^2}{S^2}} \tag{3}$$

$$\sigma = \sqrt{\frac{\sum \left(X - \overline{X}\right)^2}{S_0}} \tag{4}$$

where

U_i = Internal uncertainty

B = Average of total number of observations

σ = Standard deviation of one set of observations

S = Total number of observations

$(X - \overline{X})$ = Deviation of observations from mean

S_0 = Number of observations in one set

The sample calculations of experimental uncertainties for distillate outputs and solar intensities of the MSS during the months of April (summer) and January (winter) are listed in Tables 1 and 2, respectively. It is found that the uncertainty percentage of the distillate output and solar intensity of the MSS during summer are 2.528% and 2.470%, respectively; during winter, the corresponding values are 3.187% and 2.871%, respectively.

2.3.2. External uncertainty

The external uncertainty is mainly associated with the measuring instruments used during the experiment. This instrument uncertainty can affect the accuracy of measurement results. The various instruments used for measuring different parameters are thermocouples, thermometers, pyranometer, anemometer, and measuring jars. The associated percentage errors, accuracies, and ranges of instruments are summarized in Table 3 [19].

https://doi.org/10.1016/j.heliyon.2019.e01525

Table 1. Sample calculation of MSS experimental uncertainties in April (summer) 2017.

S. No.	Time (h)	Solar Intensity I (W/m^2)					Distillate Output (kg/m^2/h)				
		April 5	April12	April 17	April 22	April 29	April 5	April 12	April 17	April 22	April 29
1	8.00	463.00	487.00	434.00	526.00	455.00	0.00	0.00	0.00	0.00	0.00
2	9.00	657.00	698.00	661.00	723.00	596.00	0.12	0.16	0.14	0.20	0.14
3	10.00	802.00	820.00	831.00	839.00	798.00	0.37	0.39	0.40	0.46	0.40
4	11.00	838.00	848.00	809.00	843.00	844.00	0.77	0.72	0.75	0.78	0.74
5	12.00	865.00	891.00	863.00	917.00	881.00	0.92	0.86	0.90	0.93	0.89
6	13.00	821.00	790.00	802.00	793.00	799.00	0.94	0.86	0.92	0.96	0.88
7	14.00	743.00	683.00	618.00	687.00	652.00	0.88	0.80	0.84	0.88	0.81
8	15.00	542.00	509.00	501.00	516.00	491.00	0.65	0.62	0.61	0.69	0.63
9	16.00	294.00	301.00	283.00	298.00	269.00	0.44	0.42	0.44	0.48	0.42
10	17.00	90.00	98.00	83.80	119.50	107.00	0.27	0.29	0.31	0.33	0.29
11	18.00	0.30	0.14	1.30	1.20	1.60	0.20	0.18	0.18	0.21	0.16
12	19.00	0.00	0.00	0.00	0.00	0.00	0.10	0.10	0.10	0.11	0.10
13	20.00	0.00	0.00	0.00	0.00	0.00	0.07	0.07	0.07	0.08	0.07
Daily distillate output		–	–	–	–	–	5.847	5.549	5.765	6.199	5.531
Average	–	470.41	471.16	452.85	481.75	453.35	0.441	0.421	0.436	0.468	0.425
Standard deviation (σ)	–	337.11	336.69	329.61	340.59	328.64	0.334	0.305	0.322	0.332	0.316
% Uncertainty for one day		5.513	5.497	5.599	5.438	5.576	5.828	5.585	5.686	5.450	5.708
% Uncertainty for summer						2.470					2.528

https://doi.org/10.1016/j.heliyon.2019.e01525

Table 2. Sample calculation of MSS experimental uncertainties in January (winter) 2017.

S. No.	Time (h)	Solar Intensity I (W/m^2)					Distillate Output (kg/m^2/h)				
		January 3	January 9	January 13	January 17	January 24	January 3	January 9	January 13	January 17	January 24
1	8.00	188.00	214.00	241.05	185.00	217.00	0.00	0.00	0.00	0.00	0.00
2	9.00	376.00	390.00	416.72	335.00	364.00	0.02	0.01	0.03	0.02	0.02
3	10.00	561.00	501.00	574.00	504.00	543.00	0.04	0.03	0.06	0.05	0.05
4	11.00	628.00	546.00	698.55	576.00	635.00	0.16	0.15	0.18	0.16	0.16
5	12.00	686.00	598.00	701.70	605.00	679.00	0.50	0.49	0.52	0.49	0.47
6	13.00	584.00	494.00	653.90	559.00	589.00	0.55	0.56	0.57	0.53	0.56
7	14.00	467.00	366.00	521.00	408.00	498.00	0.51	0.54	0.56	0.51	0.54
8	15.00	286.00	267.00	343.00	285.00	296.00	0.49	0.46	0.51	0.48	0.49
9	16.00	122.00	79.00	156.47	116.00	113.00	0.29	0.29	0.34	0.29	0.30
10	17.00	6.03	2.08	7.69	9.17	15.00	0.16	0.14	0.18	0.16	0.14
11	18.00	0.00	0.00	0.00	0.00	0.00	0.08	0.07	0.10	0.09	0.08
12	19.00	0.00	0.00	0.00	0.00	0.00	0.06	0.04	0.07	0.06	0.07
13	20.00	0.00	0.00	0.00	0.00	0.00	0.03	0.02	0.04	0.04	0.03
Daily distillate output	–	–	–	–	–	–	2.960	2.874	3.228	2.948	3.009
Average	–	300.31	265.93	331.85	275.55	303.77	0.223	0.215	0.242	0.221	0.225
Standard deviation (σ)	–	254.17	222.02	270.49	229.53	253.38	0.207	0.211	0.215	0.201	0.208
% Uncertainty in one day	–	6.511	6.422	6.270	6.408	6.416	7.144	7.568	6.824	6.998	7.132
% Uncertainty in winter						2.871					3.187

https://doi.org/10.1016/j.heliyon.2019.e01525

Table 3. Accuracy, range, and percentage error of measuring instruments.

Sl. No.	Instrument	Accuracy	Range	% Error
1	Thermocouple	±0.1 °C	−100−200 °C	0.25%
2	Thermometer	±1.0 °C	0−100 °C	0.5%
3	Pyranometer	±1.0 W/m^2	0−1000 W/m^2	1%
4	Anemometer	±0.1 m/s	0−25 m/s	5%
5	Measuring jar	±2.0 mL	0−500 mL	2%

3. Model

3.1. Mathematical model of MSS

A mathematical model is developed for the MSS by utilizing the energy balance equations of its various parts. For the purpose of comparison, the results of the CSS theo. model from the author's previous paper are used [19].

The various heat transfer coefficients of the MSS are calculated by applying Dunkle's correlations [3]. For analysis simplification, the following assumptions are made:

(a) The heat capacities of the glass cover, jute cloth, floating thermocol, and insulating materials (sides and bottom) are neglected.

(b) There is no vapor leakage in the solar stills.

(c) Dry air and water vapor are considered ideal gases.

(d) Water flow is streamlined in the jute cloth.

(e) The temperature gradient does not change with glass cover thickness.

(f) The physical properties of various materials are constant.

The energy balance equations below are shown for MSS at different parts viz. glass cover, wetted V-shaped floating wick, and basin water as used by Srivastava and Agrawal [12].

The energy balance equations of the glass cover are the following:

$$\alpha_g\left(1-R_g\right) I + Q_{cfw-g} + Q_{efw-g} + Q_{rfw-g} = Q_{tg-a} \tag{5}$$

where

$$Q_{tg-a} = Q_{cg-a} + Q_{rg-a} \tag{6}$$

In Eq. (5), $Q_{cfw\text{-}g}$, $Q_{efw\text{-}g}$, and $Q_{rfw\text{-}g}$ denote the heat transfers through convection, evaporation, and radiation, respectively, from the floating wick to the glass cover. In Eq. (6), $Q_{cg\text{-}a}$, and $Q_{rg\text{-}a}$ are the heat transfers through convection and radiation, respectively, from the glass cover to the ambient air.

https://doi.org/10.1016/j.heliyon.2019.e01525

$$\alpha_g \left(1 - R_g\right)I + h_{tfw-g} \left(T_{fw} - T_g\right) = h_{cg-a} \left(T_g - T_a\right) + h_{rg-a} \left(T_g - T_{sky}\right) \quad (7)$$

where $h_{tfw\text{-}g}$ is the sum of the convective, evaporative, and radiative heat transfer coefficients from floating wick to glass cover; $h_{cg\text{-}a}$ and $h_{rg\text{-}a}$ represent the convective and radiative heat transfer coefficients from glass cover to ambient air; T_{fw}, T_g, T_a, and T_{sky} denote the temp. (in °C) of the floating wick, glass cover, ambient air, and sky respectively.

The energy balance equation of the V-shaped floating wick is as follows:

$$\left(1 - \alpha_g\right)\left(1 - R_g\right)\left(1 - R_{fw}\right)\alpha_{fw}I = Q_{cfw-g} + Q_{efw-g} + Q_{rfw-g} + Q_{fw-bw} \quad (8)$$

That of basin water is as follows:

$$Q_{fw-bw} = m_w c_w \left(\frac{dT_w}{dt}\right) + Q_{bw-a} \quad (9)$$

In Eqs. (8) and (9), $Q_{fw\text{-}bw}$ and $Q_{bw\text{-}a}$ define the heat transfers from the floating wick to basin water and from the basin water to ambient air through the still base, respectively. The mass (in kg) and temp. (in °C) of basin water are denoted by m_w and T_w, respectively.

From Eqs. (5), (8), and (9), the energy balance equation for the MSS can be obtained as follows:

$$\alpha_g\left(1 - R_g\right)I + \left(1 - \alpha_g\right)\left(1 - R_g\right)\left(1 - R_{fw}\right)\alpha_{fw}I = Q_{cg-a} + Q_{rg-a} + m_w c_w \left(\frac{dT_w}{dt}\right) + Q_{bw-a} \quad (10)$$

The heat transferred from the V-shaped floating wick to basin water can be written as follows:

$$Q_{fw-bw} = K_{fw} \left(T_{fw} - T_w\right) \quad (11)$$

where K_{fw} is the heat transfer coefficient of the V-shaped floating wick insulation.

The heat loss from the basin water to ambient air through the still bottom is given as follows:

$$Q_{bw-a} = h_{bw-a} \left(T_w - T_a\right) \quad (12)$$

The heat transfer phenomena occur in the MSS in two ways: internal and external. The schematic view of the heat transfer circuit in the MSS is shown in Fig. 5. The heat exchange between the wetted V-shaped floating wick surface and the inner side of the glass cover is called internal heat transfer; it occurs in three modes—convection, evaporation, and radiation. The heat transfer caused by the convection between the floating wick surface and glass cover is calculated as follows:

https://doi.org/10.1016/j.heliyon.2019.e01525

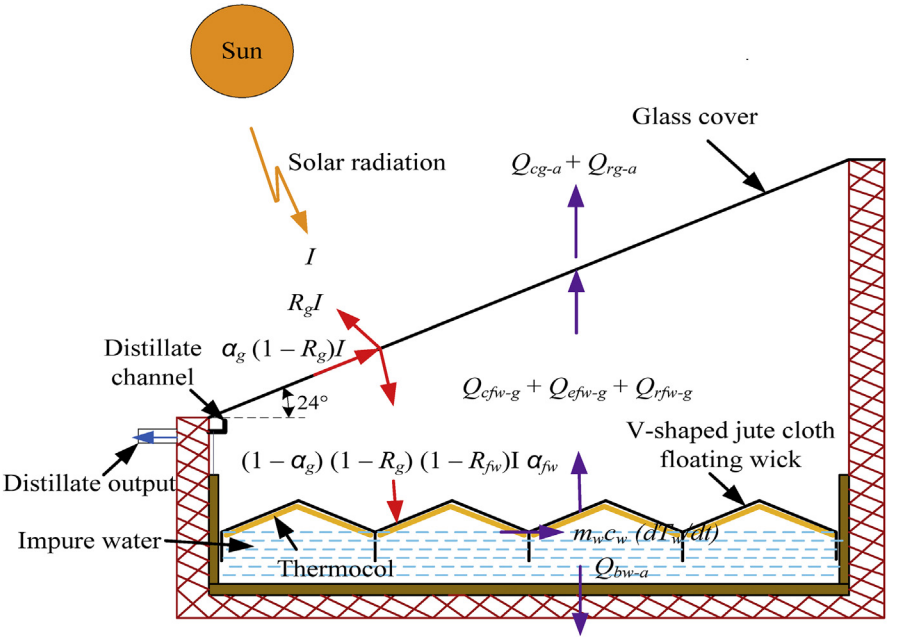

Fig. 5. Schematic view of heat transfer circuit of MSS.

$$Q_{cfw-g} = h_{cfw-g}\left(T_{fw} - T_g\right) \tag{13}$$

where h_{cfw-g} is the heat transfer coefficient caused by convection. It is given by Dunkle [3] as follows:

$$h_{cfw-g} = 0.884\left[\left(T_{fw} - T_g\right) + \frac{\left(P_{fw} - P_g\right)\left(T_{fw} + 273\right)}{\left(268.9 \times 10^3 - P_{fw}\right)}\right]^{1/3} \tag{14}$$

where p_{fw} and P_g denote the partial water vapor pressures at the floating wick temp. and glass cover temp., respectively, which are given as follows [38]:

$$P_{fw} = EXP\left\{25.317 - \frac{5144}{\left(T_{fw} + 273\right)}\right\} \tag{15}$$

$$P_g = EXP\left\{25.317 - \frac{5144}{\left(T_g + 273\right)}\right\} \tag{16}$$

The evaporative heat transfer is expressed as

$$Q_{efw-g} = h_{efw-g}\left(T_{fw} - T_g\right) \tag{17}$$

where h_{efw-g} is the evaporative heat transfer coefficient, which is given as follows [8]:

https://doi.org/10.1016/j.heliyon.2019.e01525

$$h_{efw-g} = \left(16.28 \times 10^{-3}\right) \times h_{(cfw-g)} \times \left[\frac{\left(P_{fw} - P_g\right)}{\left(T_{fw} - T_g\right)}\right] \tag{18}$$

The radiative heat transfer between the glass cover and V-shaped floating wick surface is calculated as follows:

$$Q_{rfw-g} = h_{rfw-g}\left(T_{fw} - T_g\right) \tag{19}$$

where $h_{rfw\text{-}g}$ is the radiative heat transfer coefficient of the floating wick to glass cover; it is expressed as follows:

$$h_{rfw-g} = \varepsilon_{eff}\,\sigma\left[\left(T_{fw} + 273\right)^4 - \left(T_g + 273\right)^4\right] / \left(T_{fw} - T_g\right) \tag{20}$$

The external heat transfer represents the heat loss at the top, bottom, and side walls of the solar still to the outside atmosphere.

The radiation and convection heat losses from the glass cover to the ambient air can be expressed as follows [39]:

$$Q_{rg-a} = h_{rg-a}\left(T_g - T_{sky}\right) \tag{21}$$

where the heat transfer (radiative) coefficient from the glass cover to the ambient air is given by

$$h_{rg-a} = \varepsilon_g\,\sigma\left[\left(T_g + 273\right)^4 - \left(T_{sky} + 273\right)^4\right] / \left(T_g - T_{sky}\right) \tag{22}$$

where the sky temperature (T_{sky}) given by Sharma and Mullick [40] is expressed as

$$T_{sky} = 0.0552 \times T_a^{1.5} \tag{23}$$

$$Q_{cg-a} = h_{cg-a}\left(T_g - T_a\right) \tag{24}$$

where the heat transfer (convective) coefficient from the glass cover to the ambient air is given as [41, 42].

$$(a) h_{cg-a} = 2.8 + 3.0\,V_w \text{ if } V_w \leq 5\,m/s \text{ and } 6.15 \times \left(V_w\right)^{0.8} \text{ if } V_w > 5\,m/s$$

$$(b)\; h_{cg-a} = 5.7 + 3.8\,V_w \text{ if } V_w > 5\,m/s$$

where V_w is the wind velocity in m/s.

The hourly distillate output can be expressed by the following:

$$M_{fw} = \frac{h_{efw-g} \times \left(T_{fw} - T_g\right) \times r_{fw} \times 3600}{L_{ev}} \tag{25}$$

In Eq. (25), M_{fw} represents the hourly distillate output of the MSS; L_{ev} denotes the latent heat of water evaporation, which is calculated as [43] follows:

https://doi.org/10.1016/j.heliyon.2019.e01525

$$L_{ev} = (2501.67 - 2.389 \times T_w) \times 10^3 \frac{\mathrm{J}}{\mathrm{kg}} \tag{26}$$

where

$$r_{fw} = \frac{A_{fw}}{A_b}$$

where r_{fw} can be defined as the effective surface area (evaporative) of the V-shaped floating wick per unit basin area in the MSS. The effective surface area (evaporative) of the V-shaped floating wick can also be denoted by the wick surface area on which solar radiation is received. The profile of the V-shaped black jute cloth floating wick is shown in Fig. 6. The surface area of the V-shaped floating wicks (A_{fw}) can be calculated by the following equation:

$$A_{fw} = 2hlN/\sin\theta \tag{27}$$

where "h" and "l" are the height and length of the V-shaped floating bar, respectively; "N" is the number of V-shaped floating bars; "θ" is the angle made by both legs of the V-shaped bar with respect to the horizontal. Angle "θ" is 24°, which is the same as the glass cover angle, so that the shadow effect of the V surfaces of floating wick can be minimized.

Accordingly, the daily distillate output per unit basin area is calculated as follows:

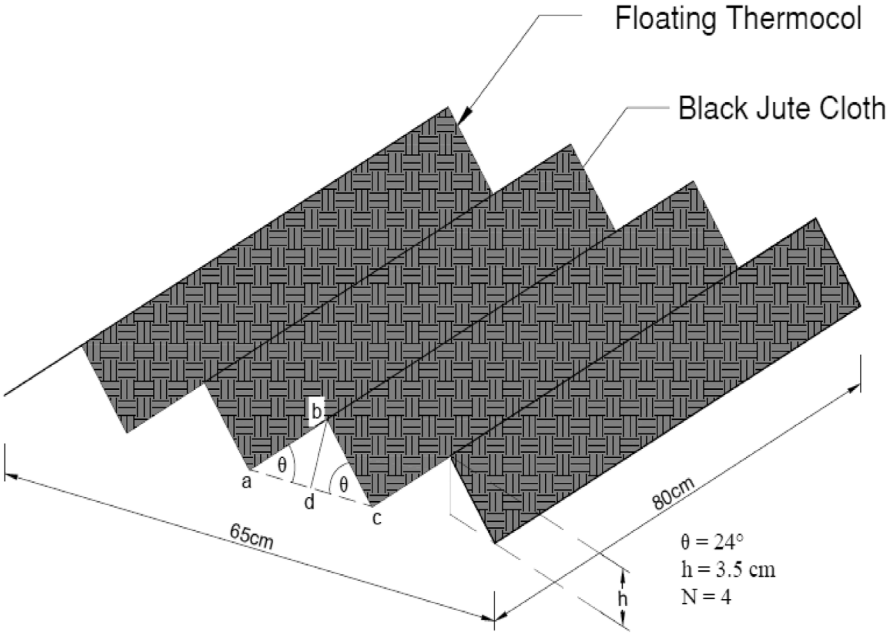

Fig. 6. Schematic view of V-shaped black jute cloth floating wick profile.

https://doi.org/10.1016/j.heliyon.2019.e01525

$$M'_{fw} = \sum_{i=1}^{24} M_{fw} \tag{28}$$

where M'$_{fw}$ is the daily distillate output (kg/m^2) of the MSS.

The instantaneous efficiency (η_i) in the case of MSS is obtained by the following relationship:

$$\eta_i = \frac{Q_{efw-g}}{I} \tag{29}$$

The overall efficiency (η_o) of the MSS can be obtained by the following:

$$\eta_o = \frac{M'_{fw} \times L_{ev}}{\sum I \times 3600} \tag{30}$$

In the MSS, the side and bottom heat losses are considerably less because the heat energy of solar radiation is not directly collected by the basin water, and its top surface is completely covered by the V-shaped floating wicks. Hence, only a small amount of heat energy is transferred to the basin water.

4. Results and discussion

During the experimentation, the readings are carefully recorded to obtain results as accurately as possible. With the help of mathematical equations, the theoretical model of MSS is developed and solved using Microsoft Excel. The required parameters for the calculations of the theo. model of the MSS are summarized in Table 4.

4.1. Effect of solar intensity and ambient air temperature variation

Fig. 7 clearly shows the variations of solar intensity (W/m^2) and ambient air temp (°C) with respect to time (h) for the clear days in summer (April 22, 2017) and winter (January 13, 2017). It is evident that the effect of solar intensity at dawn is less; it gradually increases up to a maximum range, and then decreases until sunset. For the summer and winter days, the highest solar intensity values recorded are 917 and 701.7 W/m^2 at 12:00 noon, respectively; the maximum ambient air temp. value is reached at 3:00 p.m. The time gap between the maximum solar intensity value and maximum ambient air temp. increases because of the high thermal inertia of atmospheric air. The ranges of solar intensity and ambient air temp. within 24 h are 0−917 W/m^2 and 29.5−40.93 °C, respectively, for a summer day. For a winter day, the corresponding values are 0−701.7 W/m^2 and 6.14−18.09 °C, respectively. The hourly solar intensity, ambient air temp., and wind velocity values are listed in Table 5.

https://doi.org/10.1016/j.heliyon.2019.e01525

Table 4. Design parameters of MSS.

Sl. No.	Design parameters	Numeric values
1	α_g (Condensing cover absorptivity) [44]	0.050
2	α_w (Basin water absorptivity) [44]	0.050
3	α_b (Basin liner absorptivity) [44]	0.900
4	α_{fw} (Black jute cloth floating wick absorptivity) [46]	0.850
5	R_g (Condensing cover reflectivity) [44]	0.050
6	R_w (Basin water reflectivity) [44]	0.050
7	ε_g (Condensing cover emissivity) [45]	0.940
8	ε_w (Basin water emissivity) [45]	0.950
9	ε_{eff} (Effective emittance of floating wick and condensing cover) [45]	0.820
10	C_w (Specific heat of basin water, J/kg °C) [44]	4180 J/kg °C
11	C_{fw}(Specific heat of wet jute cloth floating wick, J/kg °C) [11]	1352 J/kg °C
12	A_b (Surface area of solar still basin liner, m^2)	1 m^2
13	t_g (Thickness of condensing cover, m)	0.004 m
14	σ' (Stefan−Boltzmann constant)	5.6697×10^{-8} W/m^2 K^4
15	$h_{bw\text{-}a}$ (Coefficient of heat transfer from basin water through the base of still to ambient air, W/m^2 °C) [46]	0.77 W/m^2 °C
16	K_i (Thermal conductivity of expanded polyethylene insulation), W/m °C	0.026 W/m °C
17	t (Time, s)	3600 s
18	h (Height of V-shaped floating wick from basin water surface, m)	0.035 m
19	L (Length of V-shaped floating wick, m)	0.790 m
20	N (Number of V-shaped jute cloth floating wick)	4
21	θ (Angle between one inclined leg of floating wick to the ground)	24°

4.2. Effect of floating wick surface and basin water temperature

The theo. and exp. results of the floating wick surface and basin water temp. of the MSS and CSS for the summer and winter seasons are presented in Fig. 8. It is found that the floating wick surface temp. attains its maximum value at approximately 1:00 p.m. for the MSS; for the CSS, the basin water temp. attains its maximum value at approximately 2:00 p.m. for both seasons. The early response of heating of the floating wick in the MSS is because the thermal inertia of wetted black jute cloth is low; this is attributed to the fast increase in its temp. in the morning hours compared to the slow heating of basin water with high thermal inertia in the CSS.

https://doi.org/10.1016/j.heliyon.2019.e01525

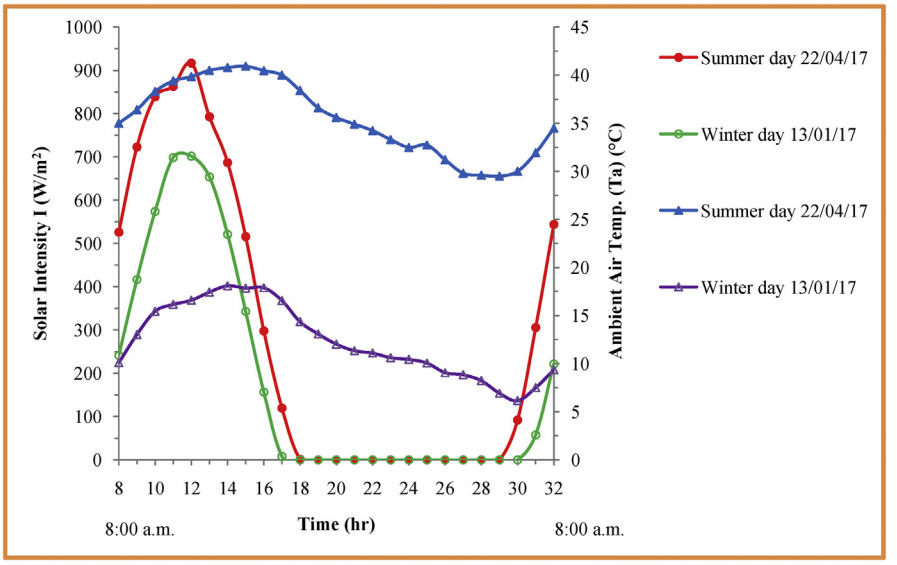

Fig. 7. Solar intensity and ambient air temp. on an hourly basis for clear summer and winter days.

The basin water temp. of the MSS in the summer and winter seasons are considerably lower than those of the CSS. Because of this, the heat losses at the sides and base of the MSS are extremely low; this results in the increase in its efficiency. Therefore, the performance of the MSS is better than that of the CSS. The maximum theo.values of the floating wick surface temp. in the summer and winter seasons are found to be 78.27 and 59.60 °C, respectively. On the other hand, in the exp. results, the corresponding values are 71.30 and 53.1 °C, respectively. The maximum theo. values of the basin water temp. for the CSS in summer and winter are found to be 71 and 66.50 °C, respectively; the maximum exp. values are 53.82 and 49.9 °C, respectively. It can be observed from the graph that the experimental values of the V-shaped jute cloth floating wick surface temp. approximates the theoretical values estimated by Dunkle's relations [3].

4.3. Effect of glass cover temperature

The variation in the theo. and exp. results of the glass cover temp. in the MSS and CSS for the summer and winter seasons is presented in Fig. 9. It can be observed that the temp. (theo. and exp.) of the glass cover is high in the case of MSS, whereas it is low in the CSS for both seasons. This is because of the large evaporating surface area and quick heating of jute cloth in the MSS than those of the CSS. According to the theo. and exp. results of the MSS, the maximum glass cover temperatures that occur at approximately 1:00 p.m. are 71.89 and 66.00 °C, respectively, in summer; in winter, the corresponding values are 46.95 and 41.97 °C, respectively. Based on the theo. and exp. results of the CSS, the maximum temperatures that occur at approximately 2:00 p.m. are 64.90 and 61.90 °C, respectively, in summer; in winter,

https://doi.org/10.1016/j.heliyon.2019.e01525

Table 5. Experimental values of solar intensity, ambient air temp., and wind velocity are presented for a summer day (April 22, 2017) and a winter day (January 13, 2017).

S. No.	Time (h)	Solar Intensity (W/m^2) Summer	Ambient Air Temp. (°C) Summer	Wind Velocity (m/s) Summer	Solar Intensity (W/m^2) Winter	Ambient Air Temp. (°C) Winter	Wind Velocity (m/s) Winter
1	08:00–09:00	526.00	35.00	02.10	241.05	10.09	01.02
2	09:00–10:00	723.00	36.40	04.64	416.72	13.03	01.31
3	10:00–11:00	839.00	38.30	3.91	574.00	15.44	01.13
4	11:00–12:00	863.00	39.40	04.58	698.55	16.15	01.87
5	12:00–13:00	917.00	39.85	03.50	701.70	16.59	01.65
6	13:00–14:00	793.00	40.50	03.85	653.90	17.44	02.61
7	14:00–15:00	687.00	40.79	05.57	521.00	18.09	02.07
8	15:00–16:00	516.00	40.93	05.21	343.00	17.85	02.35
9	16:00–17:00	298.00	40.48	03.31	156.47	17.89	01.66
10	17:00–18:00	119.50	40.00	02.91	07.69	16.56	00.58
11	18:00–19:00	01.20	38.40	00.41	00.00	14.36	02.55
12	19:00–20:00	00.00	36.60	01.43	00.00	13.09	01.74
13	20:00–21:00	00.00	35.60	01.65	00.00	12.02	01.64
14	21:00–22:00	00.00	34.90	00.93	00.00	11.34	01.13
15	22:00–23:00	00.00	34.23	01.27	00.00	11.10	00.72
16	23:00–24:00	00.00	33.30	01.85	00.00	10.62	00.68
17	24:00–01:00	00.00	32.48	02.45	00.00	10.44	01.24
18	01:00–02:00	00.00	32.74	01.92	00.00	10.06	01.22
19	02:00–03:00	00.00	31.21	02.83	00.00	09.06	01.01
20	03:00–04:00	00.00	29.80	00.57	00.00	08.84	01.11
21	04:00–05:00	00.00	29.60	02.56	00.00	08.23	01.18
22	05:00–06:00	00.00	29.50	01.42	00.00	06.92	01.40
23	06:00–07:00	91.93	30.00	01.96	00.00	06.14	00.08
24	07:00–08:00	305.80	31.93	04.55	57.55	07.50	00.03

the corresponding values are 41.75 and 38.90 °C, respectively. Evidently, the theo. and exp. values of the MSS and CSS show the same trends as indicated by the similarities of their respective graphs. In the MSS and CSS, the experimental results are found to deviate from the theoretical results by 14.25% and 16.40%, respectively.

4.4. Effect of heat transfer coefficients

The variation of heat transfer coefficients (evaporative, convective, and radiative) with time (hourly basis) in the theo. and exp. results of MSS during the summer and winter seasons are presented in Figs. 10 and 11; Dunkle's relations [3] are

https://doi.org/10.1016/j.heliyon.2019.e01525

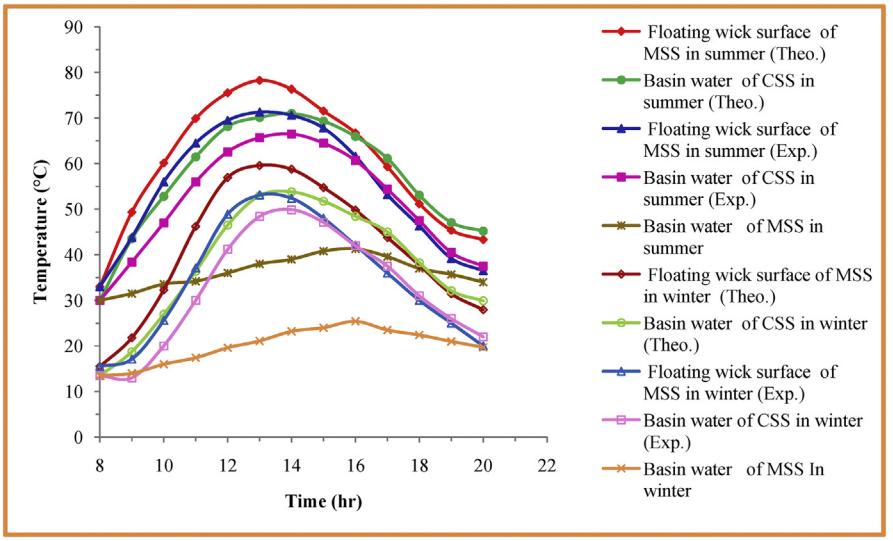

Fig. 8. Comparison of theo. and exp. values of temp. of floating wick surface and basin water surface of MSS and CSS in summer and winter on an hourly basis.

used to obtain these heat transfer coefficients. It is important to note that the theo. and exp. values of the evaporative heat transfer coefficient are significantly higher than those of the convective and radiative heat transfer coefficients. At approximately 1:00 p.m. during summer, the maximum theo. value of the evaporative, convective, and radiative heat transfer coefficients in the MSS are found to be 71.35, 2.73, and 7.81 W/m^2 °C, respectively; their maximum exp. values are 55.55, 2.67, and 7.32 W/m^2 °C, respectively. In winter, the maximum theoretical values of the evaporative, convective, and radiative heat transfer coefficients in the MSS are 29.27, 2.57, and 6.39 W/m^2 °C, respectively; their maximum exp. values are 22.08, 2.29, and 6.07 W/m^2 °C, respectively. Based on the figures, it is evident that the exp. and theo. graph trends of the heat transfer (evaporative, convective, and radiative) coefficients are significantly similar and are in close agreement.

The comparison between the theo. and exp. values of the evaporative heat transfer coefficients in the MSS and CSS during the summer and winter seasons are illustrated in Fig. 12. It can be observed that the theo. and exp. graph trends of the evaporative heat transfer coefficient in the MSS from 8:00 a.m. to 4:00 p.m. are always higher than those in the CSS; moreover, after 4:00 p.m., their trends approximate each other for both seasons. The reason for this is that compared to the slow heating rate of basin water in the CSS, the lower thermal capacity of the V-shaped floating wick surface (which is made of jute cloth) provides a quick start of heating from the morning to evening hours. Because of the high thermal capacity of basin water, more time is necessary to attain the maximum temp. point; moreover, after 4:00 p.m., its temp. range approximates that of the MSS floating wick surface.

https://doi.org/10.1016/j.heliyon.2019.e01525

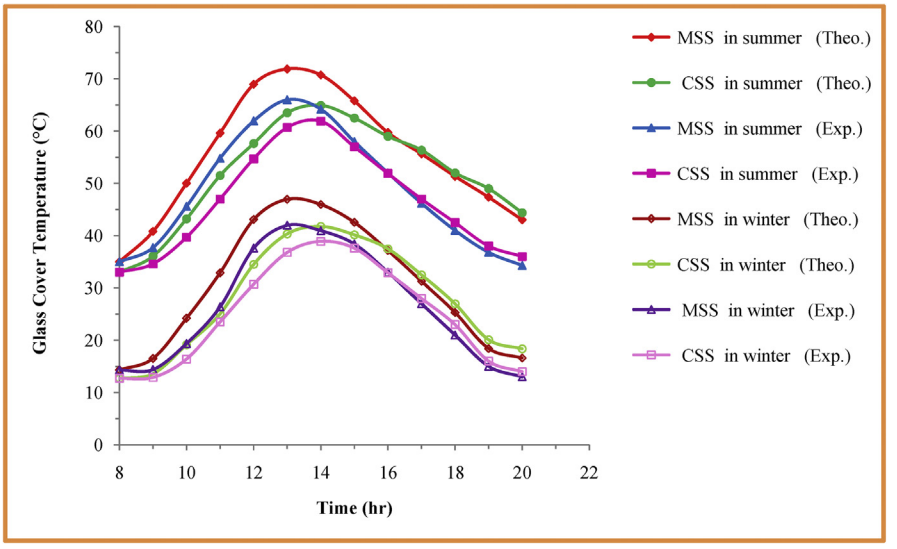

Fig. 9. Comparison of theo. and exp. values of glass cover temp. of MSS and CSS in summer and winter on an hourly basis.

4.5. Variation of hourly distillate outputs

The variations in the theo. and exp. distillate output values with time (hourly basis) in the MSS and CSS during the summer and winter seasons are shown in Fig. 13. It can be observed that the distillate output in the CSS is lesser than that in the MSS. This is because of the good evaporating properties of the jute cloth used as a floating wick material to enhance the rate of water evaporation in the MSS. The capillary property and low thermal capacity of wetted black jute cloth increase the wick

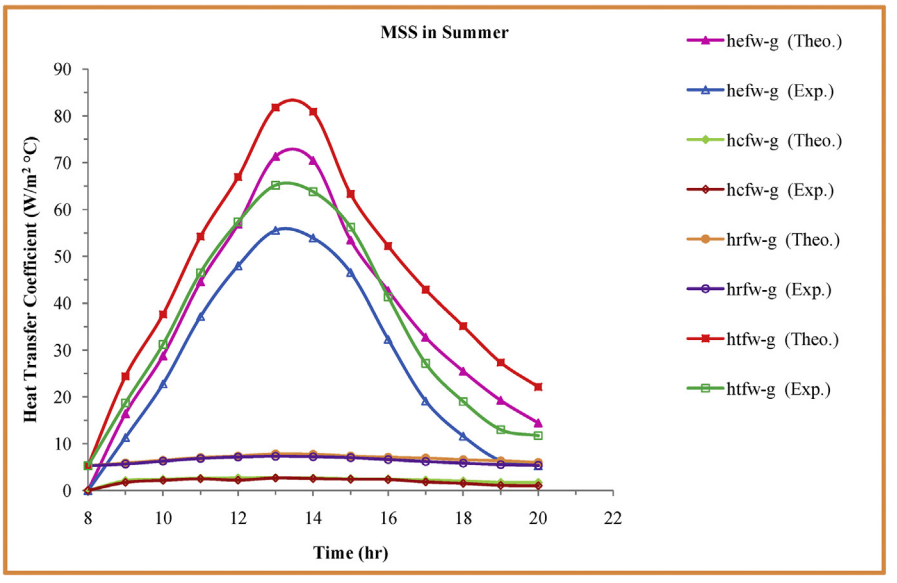

Fig. 10. Theo. and exp. values of evaporative, convective and radiative heat transfer coefficients of MSS for summer on an hourly basis.

https://doi.org/10.1016/j.heliyon.2019.e01525

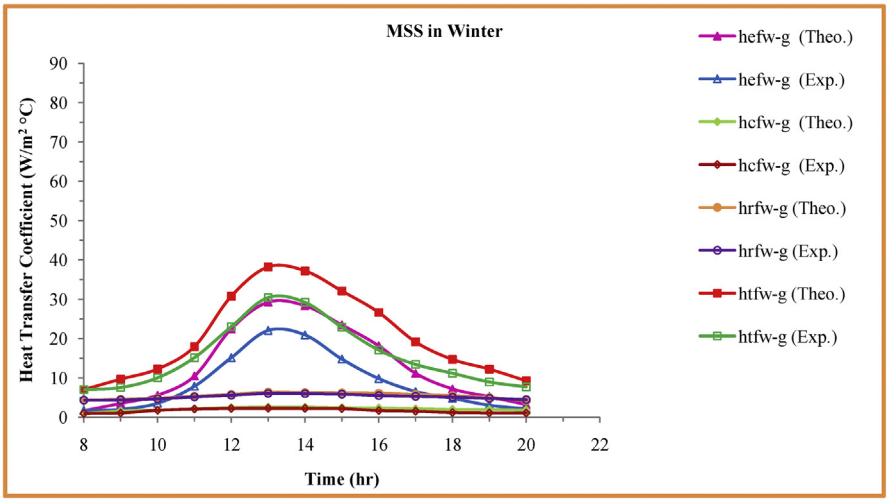

Fig. 11. Theo. and exp. values of evaporative, convective and radiative heat transfer coefficients of MSS for winter on an hourly basis.

surface temperature because more solar radiation is absorbed; consequently, the MSS has more distillate output and larger evaporating surface than the CSS. It can be observed from the figure that the maximum distillate output trends (theo. and exp. results) in the MSS occurred at approximately 1:00 p.m.; in the case of CSS, these values are obtained at approximately 2:00 p.m. because more time is required to heat the basin water. During summer, the maximum distillate output values (theo. and exp.) in the MSS are 1.11 and 0.96 kg/m^2/h, respectively; in the CSS, the corresponding results are 0.72 and 0.64 kg/m^2/h, respectively. During winter, the maximum distillate output in the MSS is found to be 0.64 and 0.57 kg/m^2/h, respectively; in the CSS, the corresponding values are 0.42 and 0.37 kg/m^2/h, respectively. It can be observed that the theo. and exp. values exhibit similar trends. The heat absorbing capacity of the wick material (black jute) can deteriorate over time as a result of salt and scale deposition on the wick surface. Hence, replacement may be necessary after a certain time (i.e., every two months); however, this replacement will not be expensive compared to that of membranes and filters in modern water purification systems.

4.6. Daily distillate output of solar stills

The theo. and exp. results of the MSS and CSS for 24 h (from 8:00 a.m. to 8:00 a.m. next day) on an hourly basis during the clear days of summer and winter seasons are shown in Fig. 14. It can be observed that in the MSS during summer, the theo. and exp. results of the cumulative distillate outputs are 45.45% and 44% higher than those of the CSS, respectively; in winter, the corresponding values in the MSS are 44.5% and 43.1% higher than those in the CSS, respectively. During summer, the theo. and exp. values of distillate outputs in the MSS are 7.36 and 6.2 kg/m^2/d; in

https://doi.org/10.1016/j.heliyon.2019.e01525

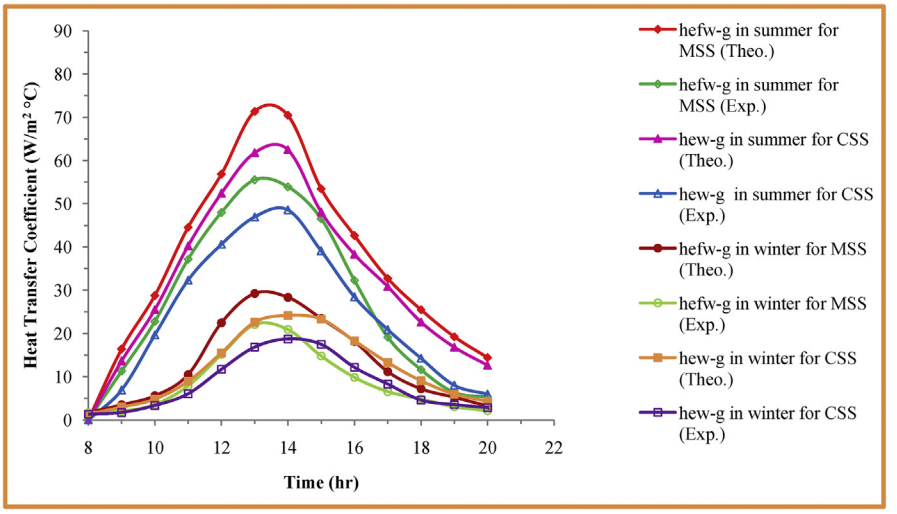

Fig. 12. Comparison of theo. and exp. values of evaporative heat transfer coefficients of MSS and CSS for summer and winter on hourly basis.

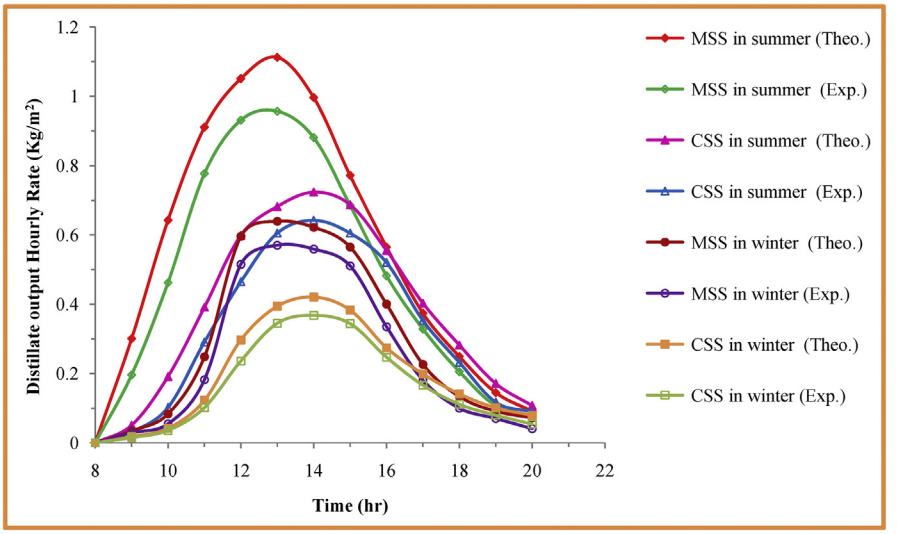

Fig. 13. Comparison of distillate output hourly rate (theo. and exp.) for MSS and CSS in summer and winter.

the CSS, the corresponding values are 5.06 and 4.23 kg/m^2/d. On a clear day in winter, the theo. and exp. values of distillate output in the MSS are 3.83 and 3.23 kg/m^2/d, respectively; the corresponding values in the CSS are 2.65 and 2.24 kg/m^2/d, respectively. These values show reasonable agreement between the theo. and exp. results of MSS and CSS.

Fig. 15 presents the day, night, and daily (theo. and exp.) distillate outputs in the MSS and CSS during the summer and winter seasons. It is observed that the maximum distillate output is obtained during daytime in both stills. The amount

https://doi.org/10.1016/j.heliyon.2019.e01525

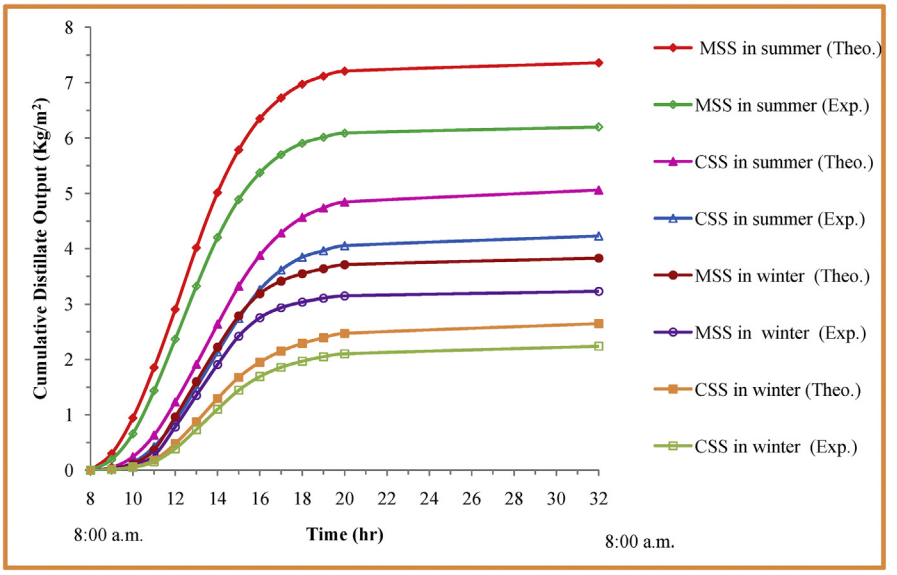

Fig. 14. Theo. values v/s exp. values of cumulative distillate output for 24 hr (8:00 a.m. to 8:00 a.m. the next day) of MSS and CSS in summer and winter.

of nocturnal distillate output in the MSS is less than that in the CSS. This corresponds to the fact that the maximum solar radiation is collected by the V-shaped floating wick surfaces, which completely cover the top surface of basin water. The floating wick is made of lightweight insulating materials (thermocol), which resist the transmission of solar radiation into the basin water; thus, less amount of heat is stored in the basin water, and thereby yields a small quantity of nocturnal distillate output in the MSS. During summer, the distillate output (theo. and exp.) values of the MSS at daytime (from 8:00 a.m. to 7:00 p.m.) are 7.21 and 6.09 kg/

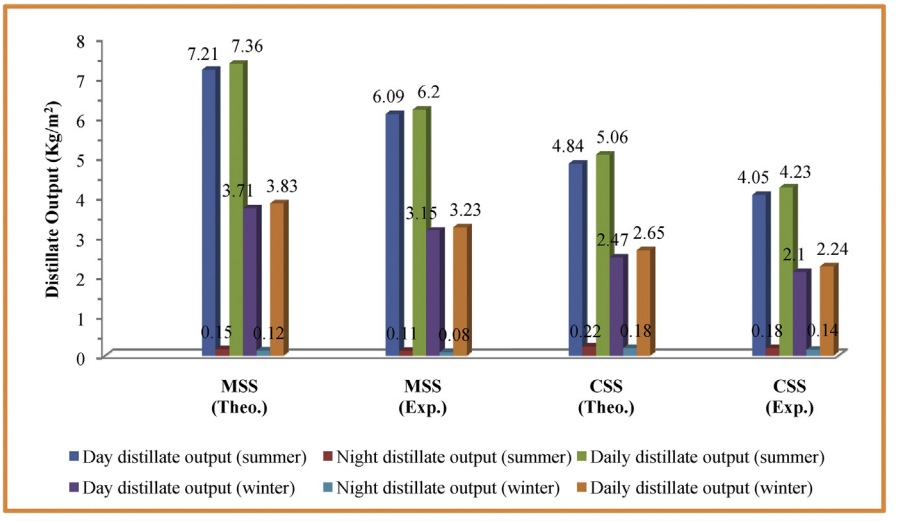

Fig. 15. Comparison of theo. and exp. values of day, night and daily distillate output of MSS and CSS in summer and winter.

https://doi.org/10.1016/j.heliyon.2019.e01525

m^2, respectively; at nighttime (from 8:00 p.m. to 7:00 a.m.), the corresponding values are 0.15 and 0.11 kg/m^2, respectively. In the case of CSS during summer, the daytime and nighttime theo. distillate output values are 4.84 and 0.22 kg/m^2, respectively; the corresponding exp. values are 4.05 and 0.18 kg/m^2, respectively. During the winter season, the theo. and exp. distillate output values of the MSS at daytime are 3.71 and 3.15 kg/m^2, respectively; the corresponding nighttime values are 0.12 and 0.08 kg/m^2, respectively.

4.7. Daily efficiency of solar stills

In Fig. 16, the theo. and exp. results of the daily efficiency of the MSS and CSS during the summer and winter seasons are compared. The theo. and exp. daily efficiency values of the MSS in summer are approximately 71.88% and 57%, respectively; for CSS, the corresponding values are approximately 47.66% and 39.84%, respectively. Similarly, the theo. and exp. daily efficiency values of the MSS during winter are approximately 56.62% and 47.75%, respectively. It can be observed that the daily efficiency of the CSS is less than that of the MSS in both the theo. and exp. cases. This is attributed to the fact that the V-shaped black jute cloth floating wicks provide additional evaporating surface area to the MSS with respect to the CSS. Moreover, the low thermal inertia and capillary property of the jute cloths increase the productivity and efficiency of the MSS.

4.8. Comparison between present and previous research works

The maximum daily distillate output values of modified solar stills that are obtained by previous researchers are compared with those of the present work, as summarized

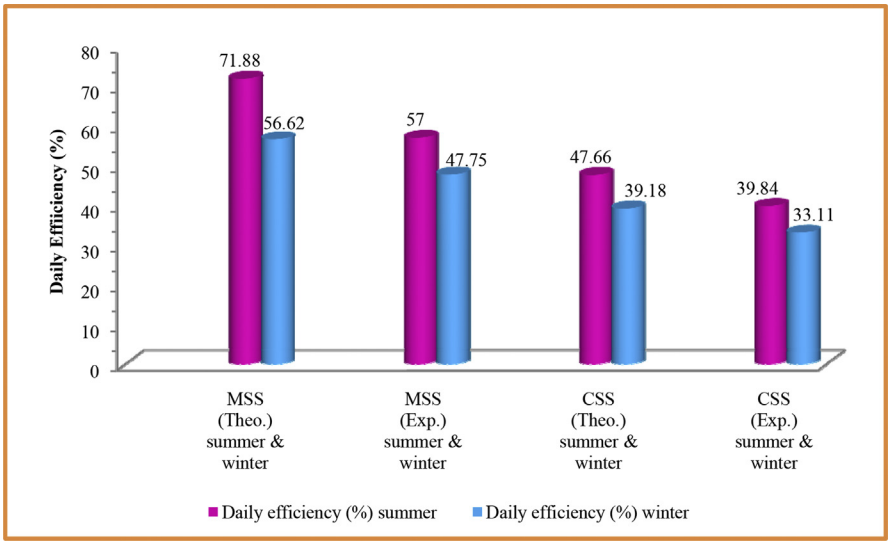

Fig. 16. Comparison of theo. and exp. values of daily efficiencies of MSS and CSS in summer and winter.

https://doi.org/10.1016/j.heliyon.2019.e01525

in Table 6. In this present research work, these values are 6.2 and 3.23 kg/m^2/d in summer and winter, respectively; these are comparable to the earlier results.

5. Analysis

5.1. Economic analysis

Solar energy is the primary input energy source to operate the solar still. The most significant advantage it affords is its zero input energy cost (solar energy). The total cost of solar stills mainly involves installation, maintenance, and operation costs. The economic analyses of the present modified and conventional solar still models are performed according to the economic analysis relations of Govind and Tiwari [47], Kumar and Tiwari [48], and Fath et al. [49]. The main purpose of this study is to assess the economic feasibility of the water purification technique for the impoverished people residing in rural and backward areas. The economic analysis is described as follows.

Let P be the initial amount invested in the solar still with the interest rate "i" per year and "n" be the useful life of solar still in terms of years for which the given solar still can perform. Then,

$$\text{Capital Recovery Factor } (CRF) = \frac{i(1+i)^n}{(1+i)^n - 1} \tag{31}$$

The first annual cost is calculated by the following relationship:

$$\text{First Annual Cost } (FAC) = (CRF) \times (P) \tag{32}$$

where P is the initial investment for the solar still.

The sinking fund factor is represented as follows:

$$\text{Sinking Fund Factor } (SFF) = \frac{i}{(1+i)^n - 1} \tag{33}$$

Therefore, the annual salvage value is given as

$$\text{Annual Salvage Value } (ASV) = (SFF) \times S' \tag{34}$$

where S' is the salvage value of the solar still.

The total annual cost (TAC) of the solar still can be calculated by considering the annual maintenance cost (AMC) and annual salvage value (ASV) as follows:

$$\text{Total Annual Cost } (TAC) = (FAC) + (AMC) - (ASV) \tag{35}$$

The annual cost of yield per kilogram (TAC/kg) can be calculated as

https://doi.org/10.1016/j.heliyon.2019.e01525

Table 6. Comparison of daily distillate output of modified single-slope single-basin solar stills using wick (present and previous research works).

S. No.	Authors	Location	Modification introduced in single slope single basin solar still	Month/Year of experiment	Maximum daily distillate output (kg/m^2/d)
1.	Al-Karaghouli & Minasian (1995) [5]	Baghdad, Iraq	Corrugated floating jute wick with reflector	January−October 1992	10.5 (summer)
2.	Sakthivel et al. (2010) [10]	Coimbatore, India	Regenerative solar still with vertical jute cloth	January−August 2006	4.00
3.	Srivastava & Agrawal (2013) [12]	Rewa, India	Multiple low thermal inertia floating porous absorbers (jute cloth)	January 2012	2.0 (winter)
4.	Matrawy et al. (2015) [14]	Taif University, Saudi Arabia	Corrugated black cloth wick with inclined reflector	May 2014	5.9
5.	Omara et al.(2016) [15]	Kafrelsheikh University, Egypt	Corrugated still with jute cloth wick (2-cm basin water depth)	May and July 2014	4.32
6.	Shalaby et al. (2016) [17]	Tanta University, Egypt	V-corrugated absorber with wick and PCM (paraffin wax)	September 2015	3.32
7.	Kaushal et al. (2017) [22]	Patiala, India	Cotton cloth floating wick basin type vertical multiple effect with heat recovery system	April−October 2016	9.89 (summer)
8.	Haddad et al. (2017) [25]	M'sila City, Algeria	Vertical rotating wick	March and June 2016	7.17 (summer) 5.03 (winter)
9.	Sellami et al. (2017) [23]	Ouargla University, southern Algeria	Basin absorber covered with blackened sponge of 0.5-cm thick sheet (polyurethane foam)	2016	4.809
10.	Arunkumar et al. (2018) [32]	Chennai, India	Porous absorber (carbon-impregnated foam) with bubble-wrap insulation	April−June, 2017	3.1
11.	Present research work	Rewa, India	V-shaped floating wicks of black jute cloth	January and April 2017	6.2 (summer) 3.23 (winter)

$$\text{Annual Cost of yield per kilogram}\left(\frac{TAC}{Kg}\right)=\frac{TAC}{Q} \tag{36}$$

where Q is the annual yield (in kg) produced by the solar still.

The market cost of yield per year is given as follows:

https://doi.org/10.1016/j.heliyon.2019.e01525

Table 7. Material cost in MSS and CSS.

S. No.	Name of material	Modified solar still			Conventional solar still		
		Quantity	Rate (Rs.)	Amount (Rs.)	Quantity	Rate (Rs.)	Amount (Rs.)
1.	Galvanized iron sheet (GI) for solar still basin	1.5 m^2	950.00/ m^2	1425.00	1.5 m^2	950.00/ m^2	1425.00
2.	Wooden box (plywood)	1 unit	1600.00	1650.00	1 unit	1650.00	1600.00
3.	Plain glass cover (4 mm thick)	1 m^2	900.00	900.00	1 m^2	900.00	900.00
4.	Expanded polyethylene sheet for insulation (8 mm thick)	3 m^2	165.00/ m^2	495.00	3 m^2	165.00/ m^2	495.00
5.	Thermocol sheet (5 mm thick)	8 m^2	90.00/ m^2	720.00	–	–	–
6.	Jute cloth	8 m^2	120.00/ m^2	960.00	–	–	–
7.	Water tank and PVC pipe fitting	1 still	1100.00	1100.00	1 still	1100.00	1100.00
8.	Paint, sealant, putty, black dye, etc.	1 still	1000.00	1000.00	1 still	1000.00	1000.00
9.	Transportation	1 still	450.00	450.00	1 still	450.00	450.00
10.	Labor charge and miscellaneous	1 still	2000.00	2000.00	1 still	2000.00	2000.00
	Total cost			10 700.00			9020.00

$$\text{Market cost of yield per year} = Q \times \text{Market cost of water per kilogram} \tag{37}$$

The net earnings per year is expressed by the following:

$$\text{Net earnings per year} = \text{Market cost of yield per year} - AMC \tag{38}$$

The payback period of solar still is given as follows:

$$\text{Payback period of solar still in days} = \frac{P}{\text{Net earnings per day}} \tag{39}$$

The experimental work is performed in the city of Rewa (located in the central part of India), where there are mainly three seasons in a year, namely rain, summer, and winter. During the rainy season, the sky is usually covered with clouds, and less solar radiation reaches the earth. As a result, the solar still cannot produce distilled water. Taking this fact into account, only approximately 250 operational days per year are included in the calculation of the yearly production of distilled water from solar stills. In the MSS, the maximum and minimum productivity values (approximately 6.2 and 2.87 kg/m^2/d, respectively) are obtained in the month of April (summer season) and January (winter season), respectively. The approximate average productivity value in one year can be estimated as 1134 kg/m^2/year. For the conventional solar still, the corresponding value is estimated as 771 kg/m^2/year. For economic analysis calculations, the annual interest rate is assumed to be 12% for 10 years of useful solar still life, as used by Kabeel et al. [50]. The material costs and the annual cost

https://doi.org/10.1016/j.heliyon.2019.e01525

Table 8. Annual cost calculation of distillate output of MSS and CSS.

S. No.	Particular	Modified solar still	Conventional solar still
1.	Initial investment (P)	Rs. 10 700.00	Rs. 9020.00
2.	Rate of interest per year (i)	12%	12%
3.	Life of still (n)	10 years	10 years
4.	Capital recovery factor (CRF)	0.177	0.177
5.	First annual cost (FAC)	Rs. 1893.73	1596.40
6.	Sinking fund factor (SFF)	0.0569	0.0569
7.	Annual salvage value (ASV) = 20% of Initial investment (P) [50]	121.94	102.80
8.	Annual maintenance cost (AMC) = 15% of FAC [50]	Rs. 284.05	Rs. 239.50
9.	Total annual cost (TAC)	Rs. 2055.84	Rs. 1733.05
10.	Annual yield produced by still (Q)	1134 kg/m^2/year	771 kg/m^2/year
11.	Annual cost of yield per kilogram	Rs. 1.81/kg	Rs. 2.24/kg
12.	Market cost of distill water per kilogram	Rs. 18.00	Rs. 18.00
13.	Market cost of distillate produced per year	Rs. 20 412.00	Rs. 13 878.00
14.	Net earnings per year	Rs. 20 127.95	Rs. 13 638.55
15.	Payback period of stillness (days)	132 days	165 days

calculations of the distillate outputs of the MSS and CSS are summarized in Tables 7 and 8, respectively.

6. Conclusions

The primary aim of this study is to increase the distillate output of conventional type solar still by introducing the V-shaped black jute cloth floating wicks. The MSS is fabricated, and experiments are conducted under the climatic conditions of Rewa, India during the summer and winter seasons. Accordingly, a mathematical model of the MSS is prepared, and its comparison is performed with respect to the exp. results. Based on the theo. and exp. studies, the following conclusions are drawn.

1. The performance of MSS is better than the CSS; this is attributed to the use of the V-shaped black jute cloth floating wicks instead of basin liner.
2. The black jute cloth and thermocol pieces are utilized in fabricating the V-shaped floating wicks. Because of the good capillary property of jute cloths, its exposed upper surface remains continuously wet as a result of the rise of basin water through the jute fiber.
3. Because of the V-shaped profile of the floating wicks, the evaporation surface area of the MSS increases by 26% compared to that of the CSS.

https://doi.org/10.1016/j.heliyon.2019.e01525

4. It is observed that the thermal capacity of the basin water in the CSS is more than that of the wet jute cloth in the MSS. Therefore, the wet jute cloth is quickly heated and reaches the maximum temp. earlier than the basin water does in the case of CSS. The exp. and theo. results exhibit good agreement.
5. The maximum glass cover temp. in the MSS is higher than that in the CSS. In the former, the maximum variation between the theo. and exp. glass cover temp. values is 14.25%; for the latter, the corresponding variation is 16.40%.
6. The evaporative heat transfer coefficients (theo. and exp.) for the MSS reach their maximum values earlier (approximately 1:00 p.m.) than the CSS does (approximately 2:00 p.m.).
7. It is observed that the CSS produces lower distillate output values compared to the MSS; this is attributed to the larger evaporation area of the V-shaped profile of floating wicks and using black jute cloths over the floating wicks. Because of low thermal inertia and good capillary property of the fabric, the distillate output amount increases.
8. The daily distillate output of the MSS is higher than that of the CSS for both the summer and winter seasons. It can be observed that an average family necessitates 25 kg of drinking water per day. This daily distillate output can be produced by four MSS units with a 1-m^2 area to satisfy the foregoing necessity by means of this environmentally friendly method. Therefore, this method may be used to provide drinking water to remote and rural areas of India where sufficient solar radiation is available in most parts throughout the year.
9. The variation between the theoretical and experimental values of parameters, such as distillate output, glass temperature, and wick surface temperature is within a reasonable limit (less than 20%).
10. It is observed that a considerably small amount of distillate is collected at night (nocturnal) in the MSS, whereas a high amount is evident in the CSS.
11. In both theo. and exp. results, the daily efficiency value in the MSS is high, whereas that in the CSS is low.
12. For a life cycle of 10 years, the annual costs of distilled water are estimated as Rs. 1.81/kg and Rs. 2.24/kg in the modified and conventional solar stills, respectively.

Declarations

Author contribution statement

Abhay Agrawal: Performed the experiments; Analyzed and interpreted the data; Contributed reagents, materials, analysis tools or data; Wrote the paper.

R.S. Rana: Conceived and designed the experiments.

https://doi.org/10.1016/j.heliyon.2019.e01525

Funding statement

This research did not receive any specific grant from funding agencies in the public, commercial, or not-for-profit sectors.

Competing interest statement

The authors declare no conflict of interest.

Additional information

No additional information is available for this paper.

Acknowledgements

The authors are extremely grateful for the support of Rewa Engineering College, Rewa, and Maulana Azad National Institute of Technology, Bhopal, M.P., India.

References

[1] G.N. Tiwari, H.N. Singh, Rajesh Tripathi, Present status of solar distillation, Sol. Energy 75 (2003) 367−373.

[2] R.K. Mall, Akhilesh Gupta, Ranjeet Singh, L.S. Rathore, R.S. Singh, Water resources and climate change: an Indian Perspective, Curr. Sci. 90 (12) (2006) 1610−1626.

[3] R.V. Dunkle, Solar water distillation: the roof type still and multiple effect diffusion still, International Developments in Heat Transfer, ASME, in: Proceedings of International Heat Transfer Conference, University of Colorado V, 1961, pp. 895−902.

[4] M.S. Sodha, A. Kumar, G.N. Tiwari, R.C. Tyagi, Simple multi wick solar still: analysis and performance, Sol. Energy 26 (1981) 127−131.

[5] A.A. Al-Karaghouli, A.N. Minasian, A floating-wick type solar still, Renew. Energy 6 (1) (1995) 77−79.

[6] Mona M. Naim, Mervat A. Abd El Kawi, Non-conventional solar stills Part 1. Non-conventional solar stills with charcoal particles as absorber medium, Desalination 153 (2003) 55−64.

[7] B.A. Abu-Hijleh, H.M. Rababa'h, Experimental study of solar still with sponge cubes in basin, Energy Convers. Manag. 44 (2003) 1411−1418.

[8] S.K. Shukla, V.P.S. Sorayan, Thermal modeling of solar stills an experimental validation, Renew. Energy 30 (2005) 683−699.

https://doi.org/10.1016/j.heliyon.2019.e01525

[9] B. Janarthanan, J. Chandrasekaran, S. Kumar, Performance of floating cum tilted-wick type solar still with the effect of water flowing over the glass cover, Desalination 190 (2006) 51−62.

[10] M. Sakthivel, S. Shanmugasundaram, T. Alwarsamy, An experimental study on a regenerative solar still with energy storage medium jute cloth, Desalination 264 (2010) 24−31.

[11] K. Kalidasa Murugavel, K. Srithar, Performance study on basin type double slope solar still with different wick materials and minimum mass of water, Renew. Energy 36 (2011) 612−620.

[12] Pankaj K. Srivastava, S.K. Agrawal, Experimental and theoretical analysis of single sloped basin type solar still consisting of multiple low thermal inertia floating porous absorbers, Desalination 311 (2013) 198−205.

[13] V. Manikandan, K. Shanmugasundaram, S. Shanmugan, B. Janarthanan, J. Chandrasekaran, Wick type solar stills: A review, Renew. Sustain. Energy Rev. 20 (2013) 322−335.

[14] K.K. Matrawy, A.S. Alosaimy, A.F. Mahrous, Modeling and experimental study of a corrugated wick type solar still: comparative study with a simple basin type, Energy Convers. Manag. 105 (2015) 1261−1268.

[15] Z.M. Omara, A.E. Kabeel, A.S. Abdullah, F.A. Essa, Experimental investigation of corrugated absorber solar still with wick and reflectors, Desalination 381 (2016) 111−116.

[16] D.G. Harris Samuel, P.K. Nagarajan, Ravishankar Sathyamurthy, S.A. El-Agouz, E. Kannan, Improving the yield of fresh water in conventional solar still using low cost energy storage material, Energy Convers. Manag. 112 (2016) 125−134.

[17] S.M. Shalaby, E. El-Bialy, A.A. El-Sebaii, An experimental investigation of a v-corrugated absorber single-basin solar still using PCM, Desalination 398 (2016) 247−255.

[18] Piyush Pal, Pankaj Yadav, Rahul Dev, Dhananjay Singh, Performance analysis of modified basin type double slope multi-wick solar still, Desalination 422 (2017) 68−82.

[19] Abhay Agrawal, R.S. Rana, Pankaj K. Srivastava, Heat transfer coefficients and productivity of a single slope single basin solar still in Indian climatic condition: experimental and theoretical comparison, Resour.Efficient Technol. 3 (2017) 466−482.

https://doi.org/10.1016/j.heliyon.2019.e01525

[20] Hitesh Panchal, Indra Mohan, Various methods applied to solar still for enhancement of distillate output, Desalination 415 (2017) 76–89.

[21] Hitesh N. Panchal, Sanjay Patel, An extensive review on different design and climatic parameters to increase distillate output of solar still, Renew. Sustain. Energy Rev. 69 (2017) 750–758.

[22] A.K. Kaushal, M.K. Mittal, D. Gangacharyulu, An experimental study of floating wick basin type vertical multiple effect diffusion solar still with waste heat recovery, Desalination 414 (2017) 35–45.

[23] M.H. Sellami, T. Belkis, M.L. Ali Ouar, S.D. Meddour, H. Bouguettaia, K. Loudiyi, Improvement of solar still performance by covering absorber with blackened layers of sponge, G. water Sustain. Dev. 5 (2017) 111–117.

[24] H. Sharon, K.S. Reddy, D. Krithika, Ligy Philip, Experimental performance investigation of tilted solar still with basin and wick for distillate quality and enviro-economic aspects, Desalination 410 (2017) 30–54.

[25] Zakaria Haddad, Abla Chaker, Ahmed Rahmani, Improving the basin type solar still performances using a vertical rotating wick, Desalination 418 (2017) 71–78.

[26] Hitesh Panchal, D.K. Patel, Prathik Patel, Theoretical and Experimental performance analysis of sandstones and marble pieces as thermal energy storage materials inside solar still, Int. J. Ambient Energy 39 (3) (2018) 221–229.

[27] Sandeepsinh Vala, Hitesh Panchal, Bhavesh Kanabar, Comparative performance evaluation of single slope and pyramid-shaped solar stills: experimental Evaluation, Int. J. Ambient Energy 39 (8) (2018) 759–766.

[28] A. Muthu Manokar, D. Prince Winston, Jayanta Deb Mondol, Ravishankar Sathyamurthy, A.E. Kabeel, Hitesh Panchal, Comparative study of an inclined solar panel, basin solar still in a passive and active mode, Sol. Energy 169 (2018) 206–216.

[29] A.E. Kabeel, S.A. El-Agouz, Ravishankar Sathyamurthy, T. Arunkumar, Augmenting the productivity of solar still using jute cloth knitted with sand heat energy storage, Desalination 443 (2018) 122–129.

[30] S. Shanmugan, S. Palani, B. Janarthanan, Productivity enhancement of solar still by PCM and Nanoparticles miscellaneous basin absorbing materials, Desalination 433 (2018) 186–198.

[31] S. Rashidi, N. Rahbar, M. Sadegh Valipour, J. Abolfazli Esfahani, Enhancement of solar still by reticular porous media: experimental investigation

https://doi.org/10.1016/j.heliyon.2019.e01525

with exergy and economic analysis, Appl. Therm. Eng. 130 (2018) 1341−1348.

[32] T. Arunkumar, A.E. Kabeel, Kaiwalya Raj, David Denkenberger, Ravishankar Sathyamurthy, P. Ragupathy, R. Velraj, Productivity enhancement of solar still by using porous absorber with bubble-wrap insulation, J. Clean. Prod. 195 (2018) 1149−1161.

[33] A.S. Abdullaha, F.A. Essa, Z.M. Omara, M.A. Bek, Performance evaluation of a humidification−dehumidification unit integrated with wick solar stills under different operating conditions, Desalination 441 (2018) 52−61.

[34] Kalpesh V. Modi, Jenish G. Modi, Performance of single-slope double-basin solar stills with small pile of wick materials, Appl. Therm. Eng. 149 (2019) 723−730.

[35] G.N. Tiwari, J.M. Thomas, Emran Khan, Optimization of glass cover inclination for maximum yield in a solar still, Heat Recovery Syst. CHP 14 (1994) 447−455.

[36] B.C. Nakra, K.K. Choudhary, Instrumentation Measurement and Analysis, first ed., Tata McGraw- Hill, New Delhi, 1985.

[37] G.N. Tiwari, M.d. Emran Khan, R.K. Goyal, Experimental study of evaporation in distillation, Desalination 115 (1998) 121−128.

[38] M.K. Gaur, G.N. Tiwari, Optimization of number of collectors for integrated PV/T hybrid active solar still, Appl. Energy 87 (2010) 1763−1772.

[39] S. Kumar, G.N. Tiwari, H.N. Singh, Annual performance of active solar distillation system, Desalination 127 (2000) 79−88.

[40] V.B. Sharma, S.C. Mullick, Estimation of heat transfer coefficients, the upward heat flow, and evaporation in a solar still, J. Sol. Energy Eng. 113 (1) (1991) 36−41.

[41] J.H. Watmuff, W.W.S. Charters, D. Proctor, Solar and wind induced external coefficients solar collectors, Technical Note, COMPLES 2 (1977) 56.

[42] J.A. Duffie, W.A. Beckman, Solar Engineering of Thermal Processes, second ed., John Wiley & Sons, New York, 1991.

[43] H.E.S. Fath, H.M. Hosny, Thermal performance of a single sloped basin still with an inherent built-in additional condenser, Desalination 142 (2002) 19−27.

https://doi.org/10.1016/j.heliyon.2019.e01525

[44] H.A. Zoori, F.F. Tabrizi, F. Sarhaddi, F. Heshmatnezhad, Comparison between energy and exergy efficiencies in a weir type cascade solar still, Desalination 325 (2013) 113–121.

[45] E. Sartori, Solar still versus evaporator: a comparative study between thermal behaviors, Sol. Energy 56 (2) (1996) 199–206.

[46] B. Janarthanan, J. Chandrasekaran, S. Kumar, Evaporative heat loss and heat transfer for open- and closed-cycle systems of a floating tilted wick solar still, Desalination 180 (2005) 291–305.

[47] J. Govind, G.N. Tiwari, Economic analysis of some solar energy systems, Energy Convers. Manag. 24 (No. 2) (1984) 131–135.

[48] S. Kumar, G.N. Tiwari, Life cycle cost analysis of single slope hybrid (PV/T) active solar still, Appl. Energy 86 (2009) 1995–2004.

[49] H.E.S. Fath, M. El-Samanoudy, K. Fahmy, A. Hassabou, Thermal-economic analysis and comparison between pyramid shaped and single-slope solar still configurations, Desalination 159 (2003) 69–79.

[50] A.E. Kabeel, A.M. Hamed, S.A. El-Agouz, Cost analysis of different solar still configurations, Energy 35 (2010) 2901–2908.

https://doi.org/10.1016/j.heliyon.2019.e01525